

Supplementary Information

**1D Topological Phase in Transition-Metal Monochalcogenides
Nanowires**

Kyung-Hwan Jin^{1,2,3}, and Feng Liu^{3,*}

¹*Center for Artificial Low Dimensional Electronic Systems, Institute for Basic Science (IBS), Pohang 37673, Korea*

²*Department of Physics, Pohang University of Science and Technology, Pohang 37673, Republic of Korea*

³*Department of Materials Science and Engineering, University of Utah, Salt Lake City, UT 84112, United States*

Corresponding Author

*E-mail: fliu@eng.utah.edu

Contents

- I. Wannier function method for 1D topological phase
- II. Topological domain wall states of extended SSH model
- III. Topological edge modes of extended SSH models
- IV. Metal-insulator transition depending on intra- and inter-hopping parameters
- V. Linear band of $\text{Mo}_4\text{Re}_2\text{X}_6$ nanowires
- VI. Atomic structure of $\text{Mo}_6\text{S}_4\text{A}_2$ (A= Cl, Br and I) nanowire and band structures
- VII. Topological domain wall states of $\text{Mo}_4\text{Re}_2\text{S}_6$ nanowire
- VIII. Correlation effect in TMM nanowires
- IX. Strain effect in TMM nanowires

I. Wannier function method for 1D topological phase

To investigate the topological properties of TMM nanowires, we calculate both the topological Zak phase and the end states using Wannier-interpolation technique. We firstly projected the Bloch wavefunction from the first-principles calculations of M_6X_6 nanowire onto $M d$ and $X p$ atomic orbitals with WANNIER90 package. WANNIER90 can optionally generate maximally localized Wannier functions (WFs) or atomic-like WF orbitals by using projection method. WFs are an orthonormal set of the spatially localized functions in a crystal that spans the same space as a specified set of Bloch bands.

The Zak phase of the n th band in a one-dimensional is directly given by the center of the WF associated with the n th band, which is defined to be the expectation value of the position operator \hat{X} of the WF. The relation between the Zak phase and the center of WF is well established in the concept of polarization in bulk crystals, and it can be developed for the topological invariants in the 1D crystals. The charge polarization is related to the position of WFs in the system, and the time-reversal polarization can be understood as the adiabatic shift of WFs. The WFs associated with lattice vector R can be written as

$$|R, n\rangle = \frac{1}{2\pi} \int_{-\pi}^{\pi} dk e^{-ik(R-x)} |u_{nk}\rangle. \quad (S1)$$

The Wannier charge center (WCC) for n -th state, \bar{x}_n , can be defined as the mean value of $\langle 0n | \hat{X} | 0n \rangle$, and $|0n\rangle$ is the state corresponding to a WF in the cell with $R=0$. Then we obtain

$$\bar{x}_n = i \int_{-\pi}^{\pi} dk \langle u_{nk} | \partial_k | u_{nk} \rangle =: P_n. \quad (S2)$$

This form is exactly same as the Zak phase of n -th state and it can be shown that the sum of WCCs of all the occupied bands for a multi-band system corresponds to the total Zak phase φ_{Zak} . We note that there is a fundamental relation between the Zak phase the the polarization P of a 1D system.

II. Topological domain wall states of extended SSH model

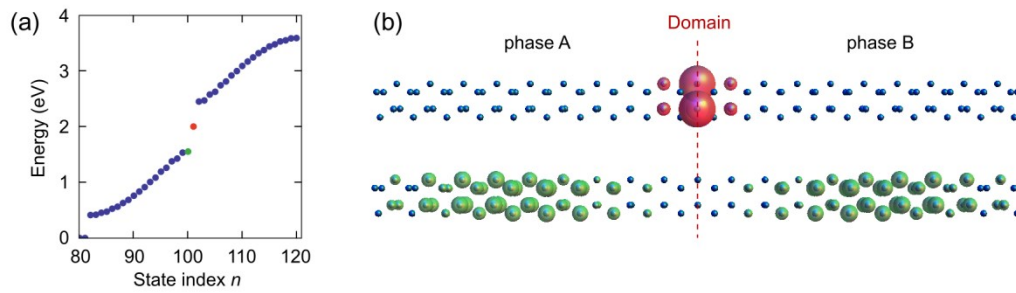


Figure S1. (a) The calculated discrete energy levels of extended SSH model [Fig. 1(c)] with domain walls between phase A and phase B. Topological domain wall states (bulk states) are indicated by red (green) dots. (b) The charge distribution of topological domain walls (red spheres) states and bulk states (green spheres) indicated by number in (a), respectively.

III. Topological edge modes of extended SSH models

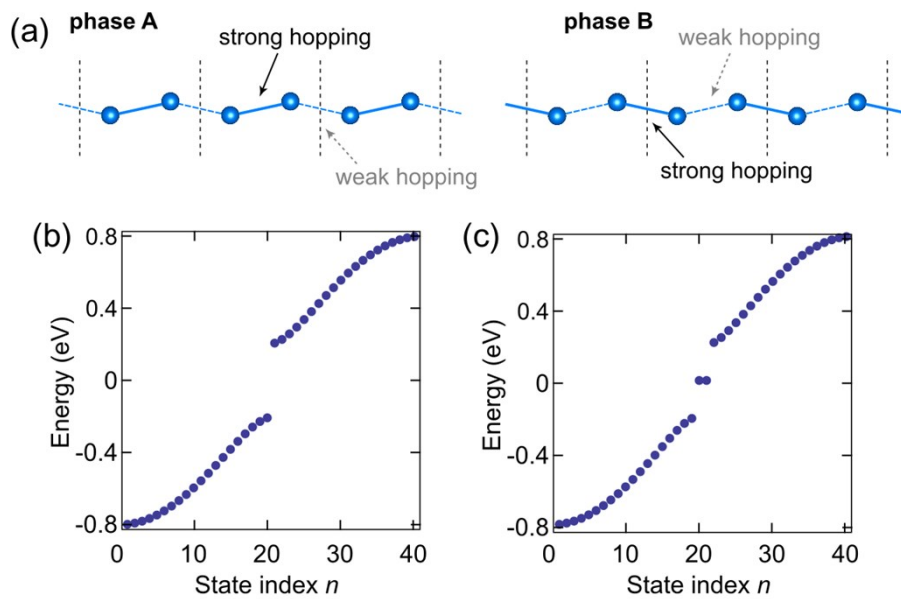


Figure S2. (a) The two phases in the SSH model where the strong hopping is either inside the unit cell (phase A) or between the unit cells (phase B). (b) The calculated edge states of finite chain for phase A ($t=0.4$ eV and $\delta=0.1$ eV) and phase B ($t=0.4$ eV and $\delta=-0.1$ eV) in (a), respectively. The finite chain length is 40 times of unit cell.

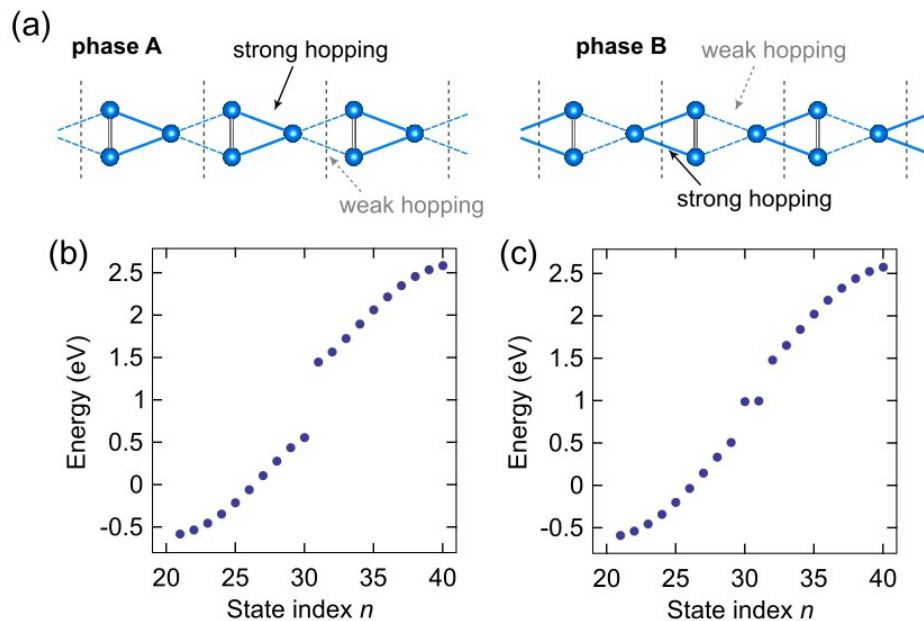


Figure S3. (a) The two phases in the extended SSH model with four-atom basis where the strong hopping is either inside the unit cell (phase A) or between the unit cells (phase B). (b) The calculated energy states of finite chain for phase A ($t=0.4$ eV, $t_m=1$ eV and $\delta=0.1$ eV) and phase B ($t=0.4$ eV, $t_m=1$ eV and $\delta=-0.1$ eV) in (a), respectively. The finite chain length is 20 times of unit cell.

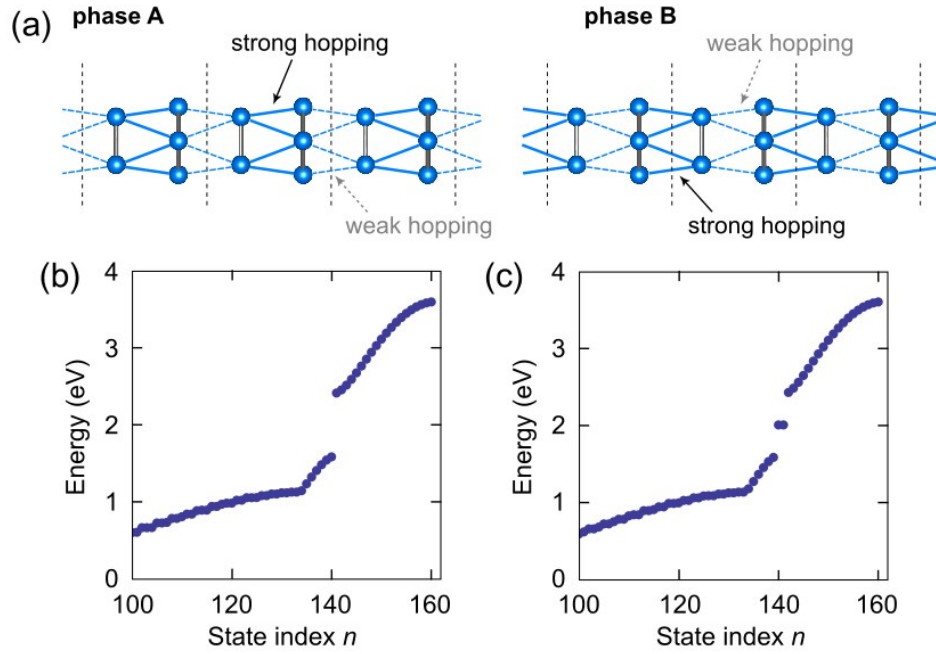


Figure S4. (a) The two phases in the extended SSH model with eight-atom basis where the strong hopping is either inside the unit cell (phase A) or between the unit cells (phase B). (b) The calculated energy states of finite chain for phase A ($t=0.4$ eV, $t_m=1$ eV and $\delta=0.1$ eV) and phase B ($t=1$ eV, $t_m=0.4$ eV and $\delta=-0.1$ eV) in (a), respectively. The finite chain length is 20 times of unit cell.

IV. Metal-insulator transition depending on intra- and inter-hopping parameters

M_6S_6 and M_6Se_6 nanowires show metallic character, whereas M_6Te_6 is insulating. The metal-insulator transition can be explained by TB model. In the Eq. (1), there are two hopping parameters. One is the inter-molecular hopping t and the other is the intra-molecular hopping t_m . Depending on the ratio of these parameters, there are two types of band structure. If the parameters satisfy the condition $t > t_m/2$, the conduction band overlaps the valence band and forms metallic states near the Fermi level. If $t = t_m/2$, the parabolic bands at the Γ point are touched and the band gap is closed. When $t < t_m/2$, the 1D system has the insulating band [Fig. S5].

For the hopping parameters in TMM nanowires, the bonding distances between inter M-M atoms d_{inter} and intra M-M atoms d_{intra} are checked [Table S1]. Typically, the hopping parameter is inversely proportional to d^2 . As halogen atomic mass increases, the ratio of inter bonding length to intra bonding length ($d_{\text{inter}}/d_{\text{intra}}$) is increased. Effectively, the inter-molecular hopping t is decreased for the M_6Te_6 nanowires. This is the reason for the metal-insulator transition of TMM nanowires.

Table S1. The bonding distance between inter M-M atoms d_{inter} and intra M-M atoms d_{intra} .

	d_{inter}	d_{intra}	$d_{\text{inter}}/d_{\text{intra}}$
Mo_6S_6	2.692	2.485	0.9806
Mo_6Se_6	2.724	2.618	0.9960
Mo_6Te_6	2.758	2.816	1.0365
W_6S_6	2.703	2.515	0.9811
W_6Se_6	2.731	2.678	0.9988
W_6Te_6	2.759	2.874	1.0257

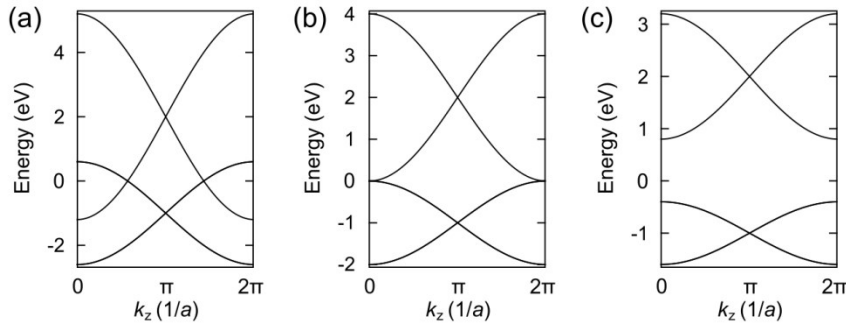


Figure S5. Tight binding band structures of extended SSH model with six-atom basis with parameter: (a) $t=0.8$ eV, $t_m=1$ eV; (b) $t=0.5$ eV, $t_m=1$ eV; (c) $t=0.3$ eV, $t_m=1$ eV, respectively.

V. Linear band of $\text{Mo}_4\text{Re}_2\text{X}_6$ nanowires

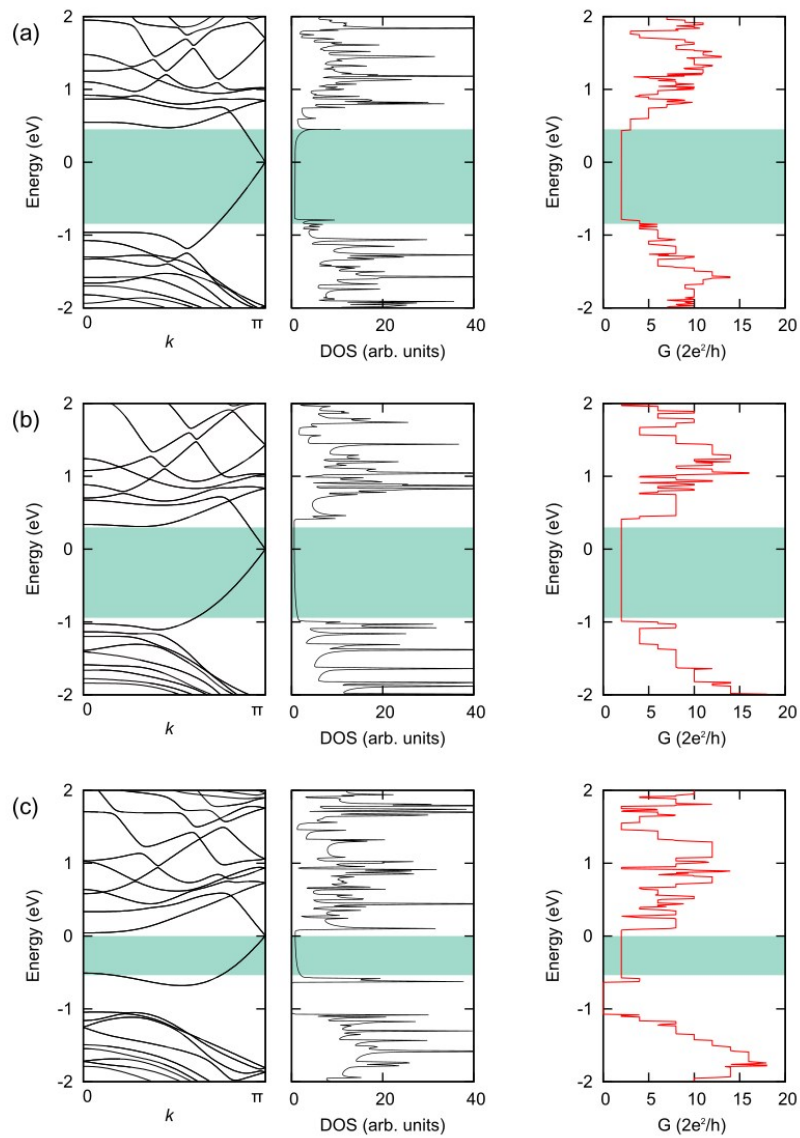


Figure S6. (a) The calculated band structure, DOS and quantum conductance G of the $\text{Mo}_4\text{Re}_2\text{S}_6$ nanowire, respectively. (b),(c) Corresponding quantities of the $\text{Mo}_4\text{Re}_2\text{S}_6$ and $\text{Mo}_4\text{Re}_2\text{Se}_6$ nanowire, respectively. Constant DOS and conductance near Fermi level is originated from 1D Dirac band.

VI. Atomic structure of $\text{Mo}_6\text{S}_4\text{A}_2$ (A= Cl, Br and I) nanowire and band structures

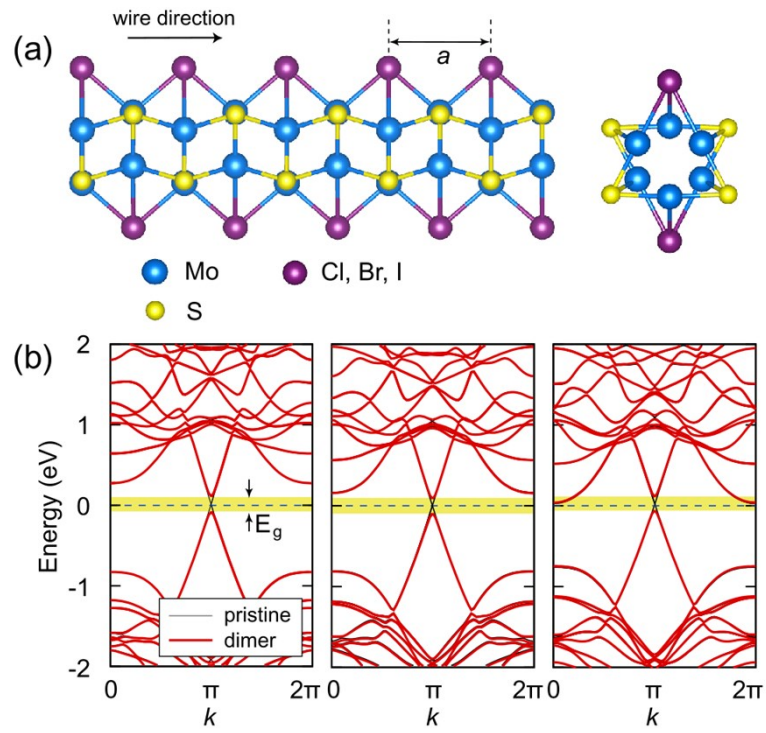


Figure S7. (a) Atomic structure of the $\text{Mo}_6\text{S}_4\text{A}_2$ (A= Cl, Br and I) nanowire. (b) The calculated band structure of $\text{Mo}_6\text{S}_4\text{A}_2$ (from left to right, A= Cl, Br and I) nanowires, respectively.

VII. Topological domain wall states of $\text{Mo}_4\text{Re}_2\text{S}_6$ nanowire

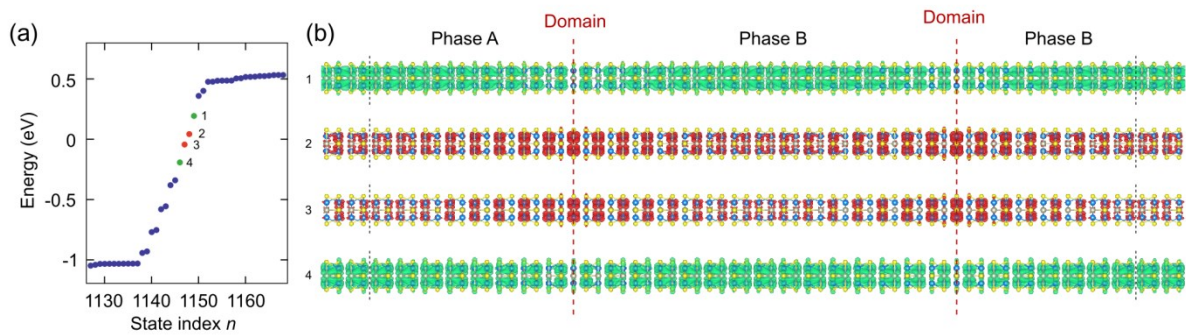


Figure S8. (a) The calculated discrete energy levels of supercell of $\text{Mo}_4\text{Re}_2\text{S}_6$ nanowire with domain walls between phase A and phase B. Topological domain wall states (bulk states) are indicated by red (green) dots. (b) The real-space charge distribution of topological domain walls states and bulk states indicated by number in (a), respectively.

VIII. Correlation effect in TMM nanowires

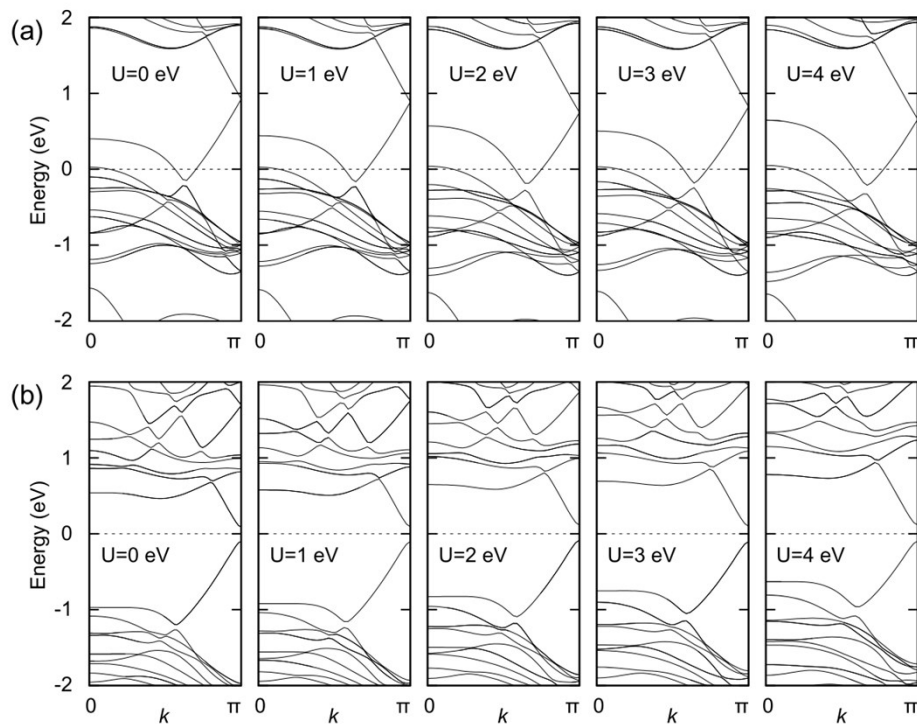


Figure S9. The calculated band structures of (a) Mo_6S_6 and (b) $\text{Mo}_4\text{Re}_2\text{S}_6$ nanowire using different U values from 0 to 4 eV for Mo and Re atoms.

IX. Strain effect in TMM nanowires

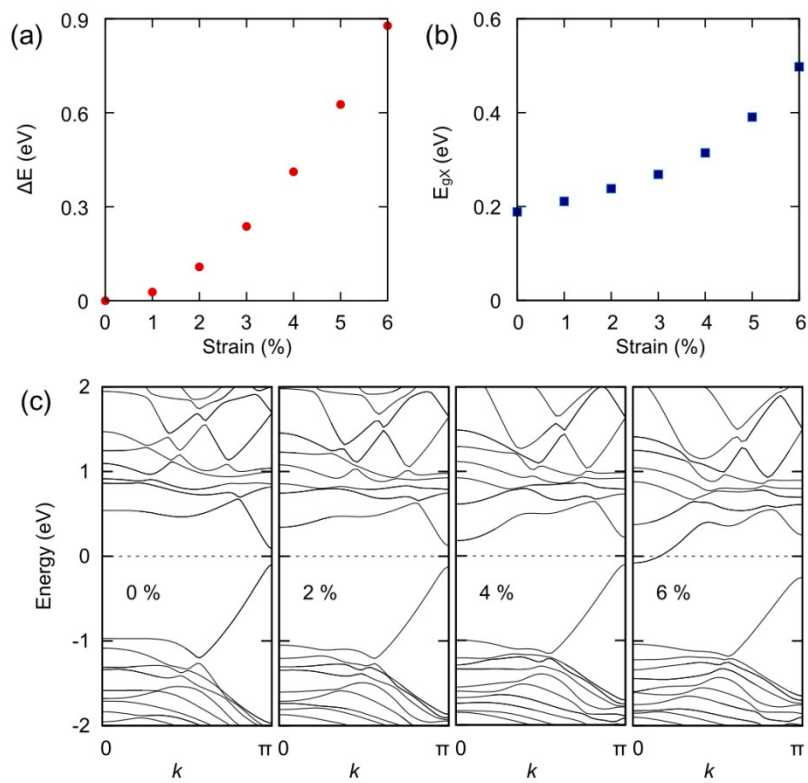


Figure S10. (a) Energy and (b) energy gap at X point of $\text{Mo}_4\text{Re}_2\text{S}_6$ nanowire as a function of axial strain. (c) Calculated band structures with different strains.